

Modal Evaluation of Reinforced Cement Concrete Tall Buildings Using ETABS

Kashyap Shukla⁽¹⁾, Nallasivam Kanagaraj^(1*)

⁽¹⁾ Department of Civil Engineering, National Institute of Technology (NIT) Hamirpur 177001, Himachal Pradesh, INDIA
e-mails: 20mce109@nith.ac.in; nallasivam@nith.ac.in*

SUMMARY

The planning and construction of tall buildings are regulated by lateral forces such as seismic and wind loads. It is imperative to perform a modal analysis of the framework before performing the dynamic evaluation of the building when subjected to lateral forces. Consequently, building professionals focus on calculating the inherent frequency and associated natural period in tall structures to assess the vibrational behaviour of the building's frame. The current research aims to investigate and evaluate the performance of various tall building frameworks with differing shear wall configurations under free vibration, as the arrangement of shear walls significantly influences the stability of the structure against lateral forces. This investigation employs the eigenvalue estimation method for examining rectangular buildings with various shear wall configurations using the FEM program ETABS. The outcomes of this research include predictions of the natural frequency and mode shape for numerous tall rectangular building simulations with numerous configurations of shear wall components by modal simulation. The natural frequency range, time period, mode shapes, and mass participation factors were extracted from the data.

As the model's stiffness increases due to the incorporation of shear wall, the natural time period diminishes across each configuration It is imperative to perform. The model incorporating centrally positioned shear walls in a core configuration demonstrated a 35% reduction in the fundamental time period compared to rectangular structures without shear walls. The investigation is restricted to the modal evaluation of tall rectangular building frameworks and does not include uncertainty quantification (UQ).

KEY WORDS: *high-rise building; Finite Element Method; ETABS simulations; free vibration; eigenvalue.*

1. INTRODUCTION

Humankind's interest in tall building construction dates back to ancient times. Therefore, when the urban population grows fast, high-rise construction becomes a necessity. As a result, there is considerable potential for research and development in the field of high-rise construction. Structural analysts define a tall structure as one that experiences lateral forces due to wind or

seismic activity, which significantly influence its structural design [1]. Modal evaluation has garnered significant attention in the last century for numerous applications. In this scenario, it is essential to ascertain the fundamental characteristics of tall buildings, including vibration modes, inherent frequencies, natural periods, as well as aspects such as modal orientation variables and mass participation factors. Sultan and Peera [2] utilized ETABS to produce mode shape simulations demonstrating various building configurations under dead load, subsequently employing dynamic analysis for evaluating story shear, story drift, and overturning moments. Malekinejad and Rahgozar [3] developed a computational simulation of a tall building incorporating an outrigger-belt truss to determine its mode shapes and natural frequencies. Lorenzo et al. [4] investigated the random response of a 22-story concrete superstructure via operational modal evaluation. Rahgozar [5] determined the inherent frequency of diverse tall building constructions incorporating shear cores, outrigger systems, framed tubes, and belt trusses. The mathematical model for the vibration-free building has been developed employing the Hamiltonian variational principal. Maison and Ventura [6] determined the fluctuating response of a thirteen-story building and compared the outcomes with real data extracted from earthquake recordings during two actual seismic events. Ozyigit [7] examined frames using FEA and undertaken simultaneous free and forced in-plane and out-of-plane vibration analyses of the frameworks. The frames featured circular sections with either straight or curved segments. Awkar and Lui [8] employed a numerical simulation to explore the responses of multi-story flexibly connected frames to seismic excitations. Geometric and material variations were incorporated in the simulation analyses. Kwon and Bang [9] employed FEM to determine the inherent frequencies of trusses, Euler beams, Timoshenko beams, and frame elements. They compared the FEM outcomes for natural frequencies with those acquired through theoretical methods. In a paper, Jang and Bert [10] examined the modal performance of a stepped beam. He investigated the minimal natural frequency of a stepped beam with two distinct cross-sections under diverse boundary conditions. Blevins's study [11] was highly beneficial in understanding the principles of natural frequency and mode shapes, two essential concepts in vibration research. Klein [12] investigated the free vibration of beams characterized by elastic and non-uniform properties using a novel method that integrates the benefits of both the FEM and Rayleigh-Ritz analysis. In his article, Gladwell [13] determined the inherent frequencies and basic patterns of undamped vibrations of a planar framework built from a grid of rectangles of identical beams. Verma and Nallasivam [14], [15], and [16] implemented the vibration analysis of the box-girder bridge through free vibration and static simulation combining MATLAB computing and ANSYS. The present investigation aims to ascertain the modal response of tall structures, which particularly requires modelling prior to undertaking dynamic simulations due to vibrational forces generated by seismic activity. This paper utilizes ETABS tools [17] for simulating the natural vibration behaviour of high-rise structures through an analysis of parameters associated with different shear wall configurations.

2. FEM MODELLING OF MULTI-STORY HIGH-RISE BUILDING RESULTS AND DISCUSSION

The initial segment of the investigation involves the simulation of multi-story high-rise buildings. Nine G+30-story frameworks have been developed using the ETABS FEM simulation programme. The initial model is a rectangular structure without shear walls, but the subsequent eight models include various shear wall configurations within rectangular structures. Figures 1-9 illustrate all of these simulations, with details concerning the configuration of shear walls in each model provided below (from Simulation 1 to Simulation 9):

- Simulation - 1: Rectangle structure without shear walls (Figure 1)
- Simulation - 2: Structure incorporating shear walls positioned at each of the four corners-1 (Figure 2)
- Simulation - 3: Structure incorporating shear walls positioned at each of the four corners-2 (Figure 3)
- Simulation - 4: Structure incorporating shear walls positioned solely at two opposing corners (Figure 4)
- Simulation - 5: Structure incorporating shear walls positioned at each of the four edges (Figure 5)
- Simulation - 6: Structure incorporating a centrally positioned shear wall as the core (Figure 6)
- Simulation - 7: Structure incorporating shear walls positioned at two opposing corners at the centre (Figure 7)
- Simulation - 8: Structure incorporating a centrally positioned shear wall in an E-shaped configuration (Figure 8)
- Simulation - 9: Structure incorporating a centrally positioned shear wall in an I-shaped configuration (Figure 9)

2.1 DIMENSIONAL CONFIGURATIONS MATERIAL PROPERTIES

A three-dimensional model has been established extending along gridlines 10 and 7, aligned with the Y and X directions, respectively, comprising 31 levels. The beams and columns are categorized as one-dimensional frame elements, whereas slabs and shear walls are characterized as two-dimensional shell elements. Table 1 presents the dimensional details of each element. The total length of the shear wall in the floor plan is consistent across all variants; only the positioning varies.

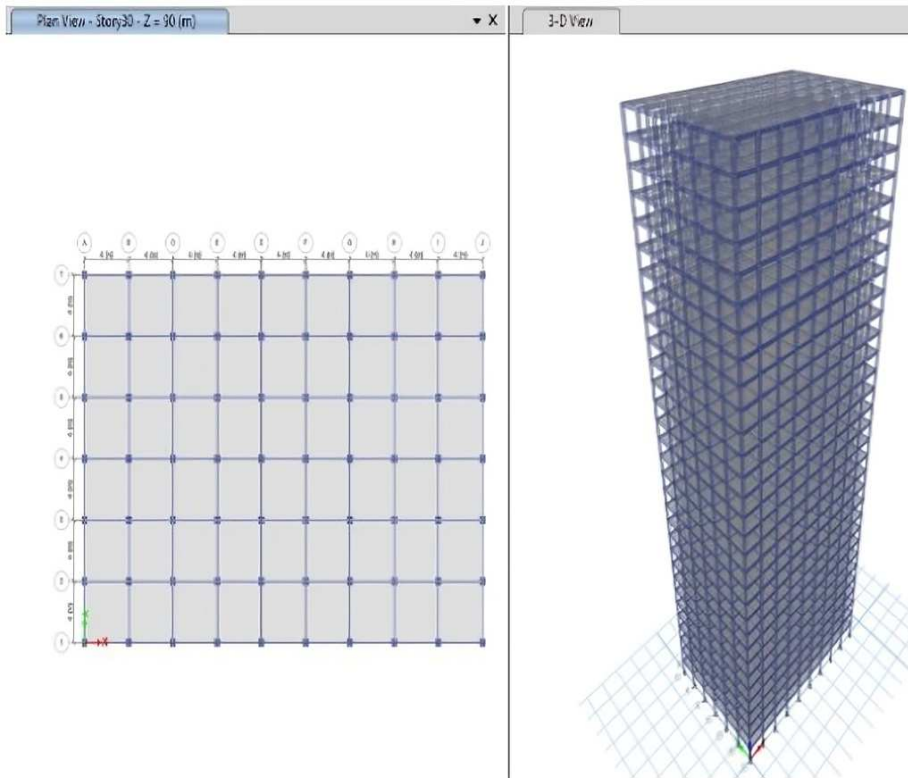


Fig. 1 Simulation 1 - Structure absent of shear walls

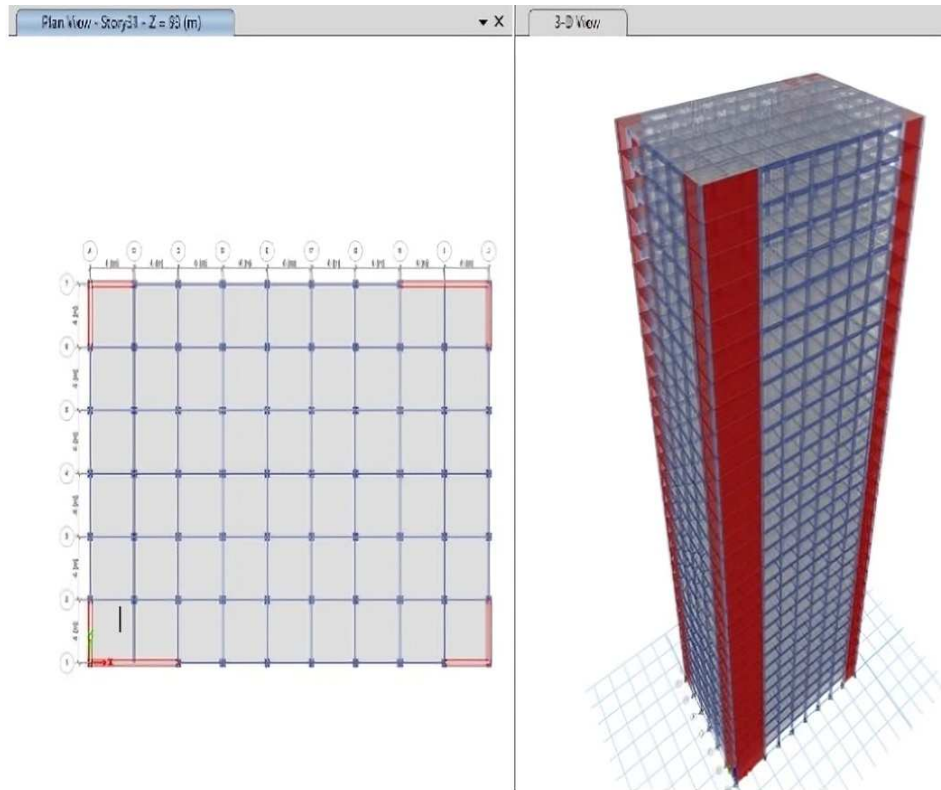


Fig. 2 Simulation 2 - Structure incorporating shear walls positioned at each of the four corners - 1

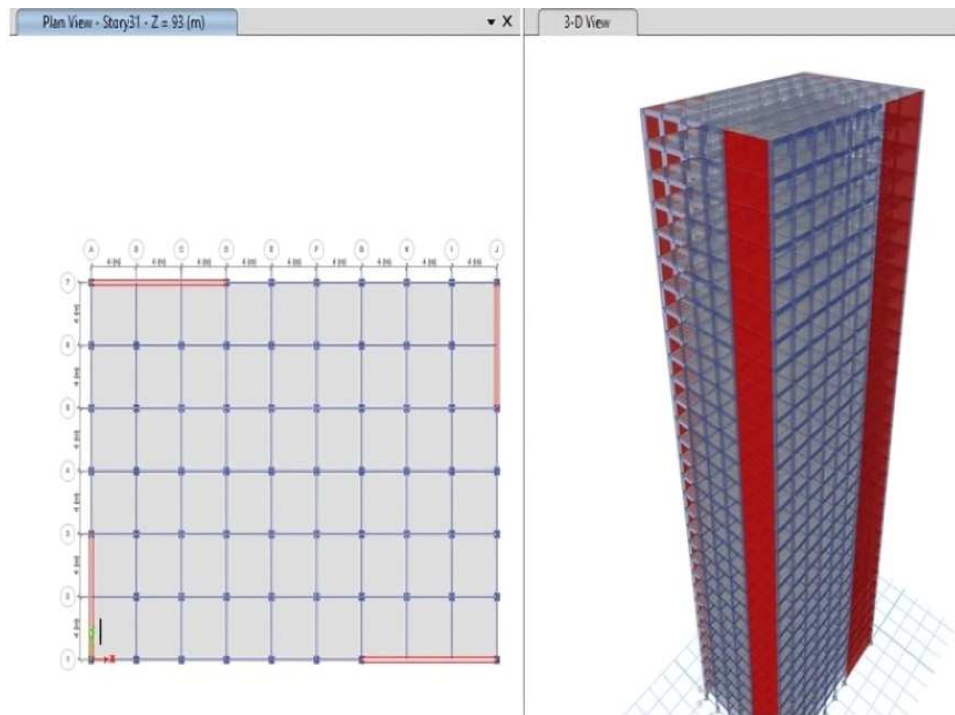


Fig. 3 Simulation 3 - Structure incorporating shear walls positioned at each of the four corners - 2

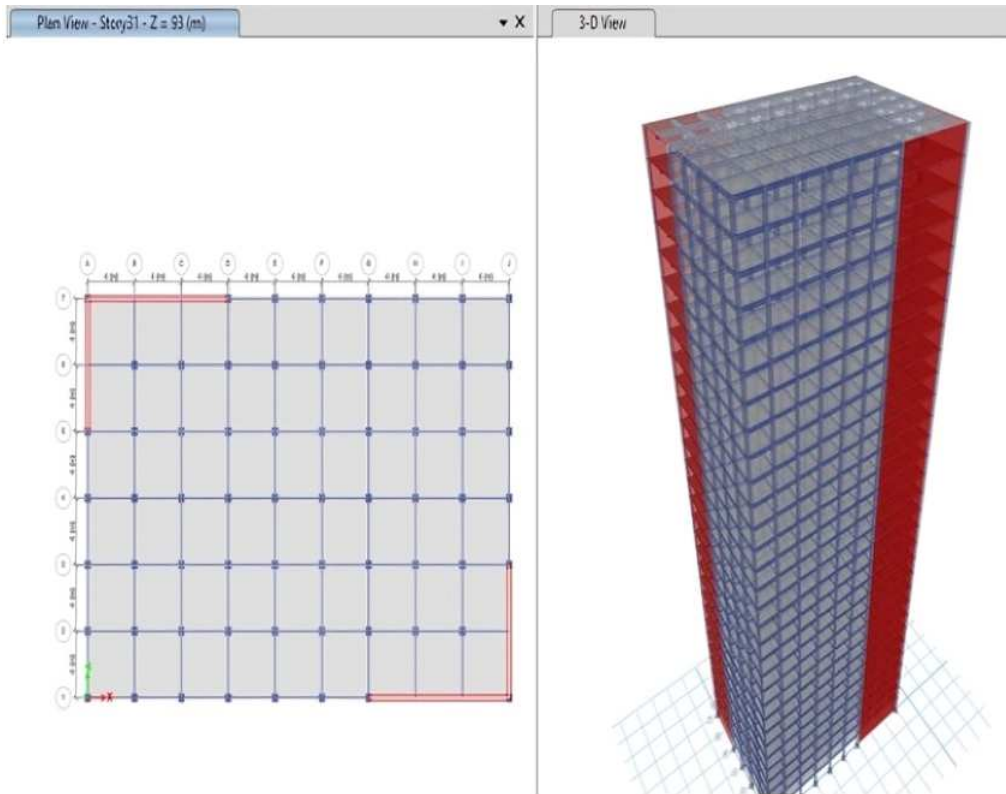


Fig. 4 Simulation 4 - Structure incorporating shear walls positioned solely at two opposing corners

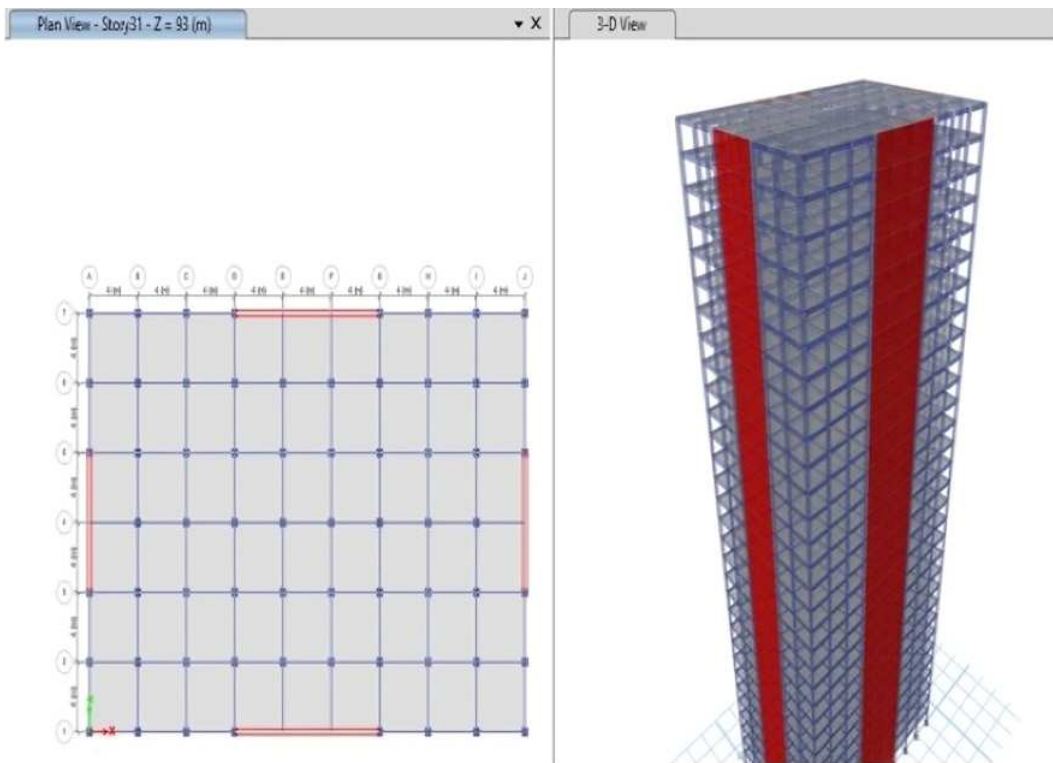


Fig. 5 Simulation 5 - Structures incorporating shear walls positioned at all four peripheries

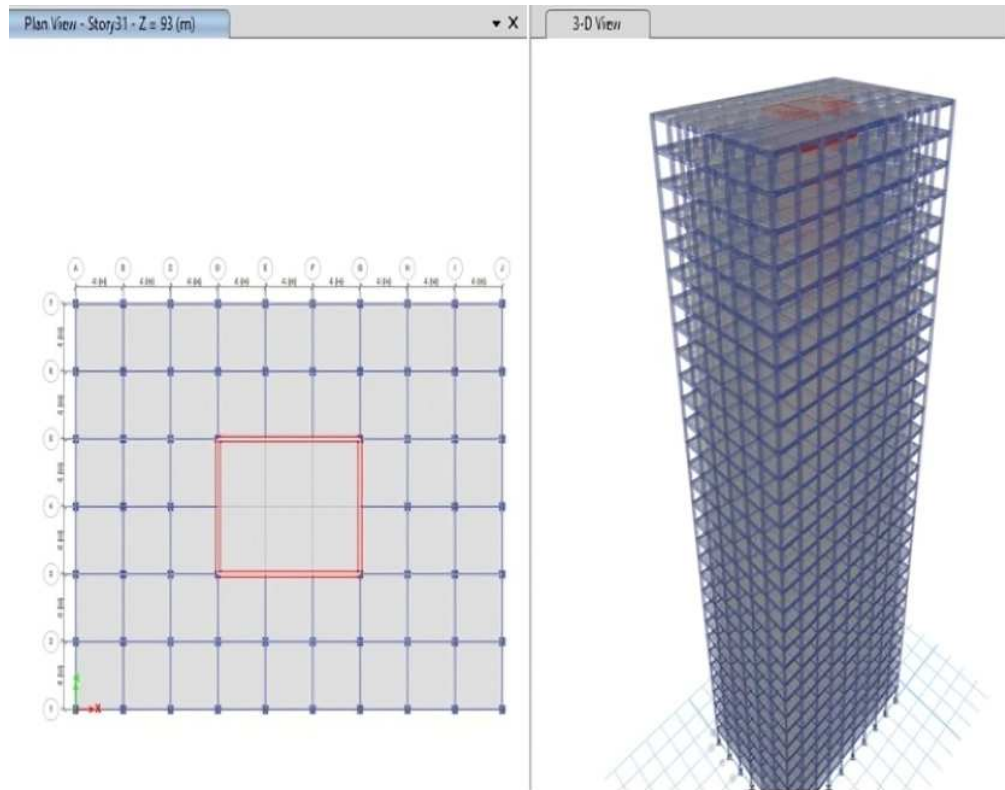


Fig. 6 Simulation 6 - Structures incorporating a centrally positioned shear wall as the core

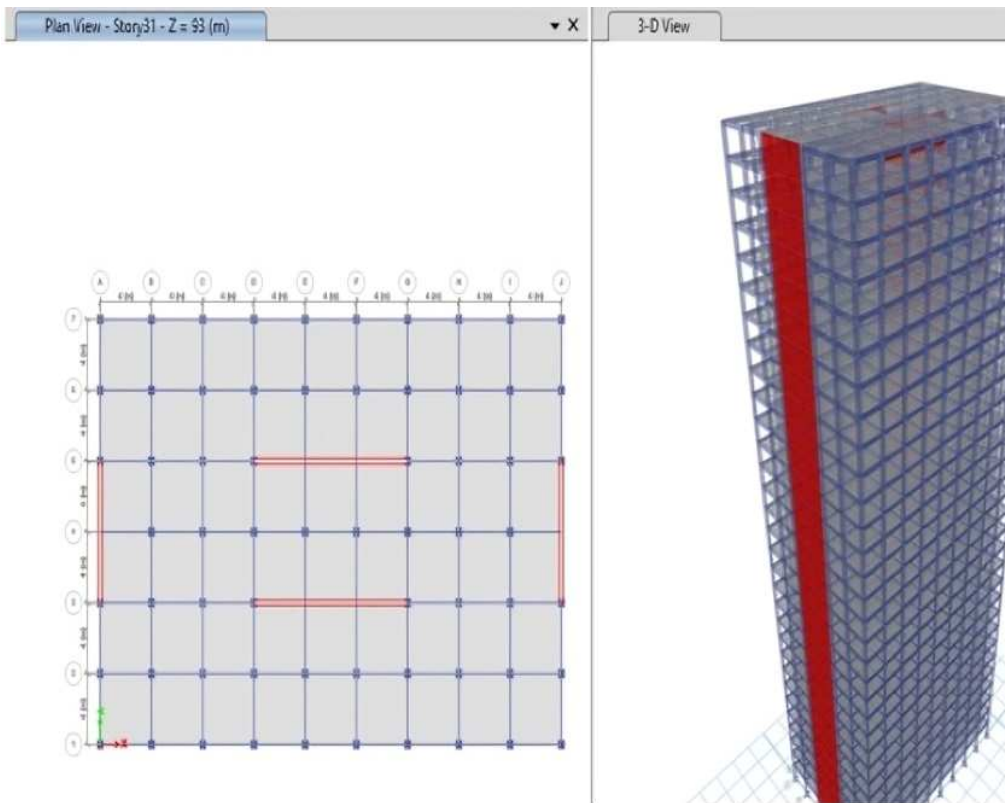


Fig. 7 Simulation 7 - Structure incorporating shear wall positioned at two opposing edges and centre

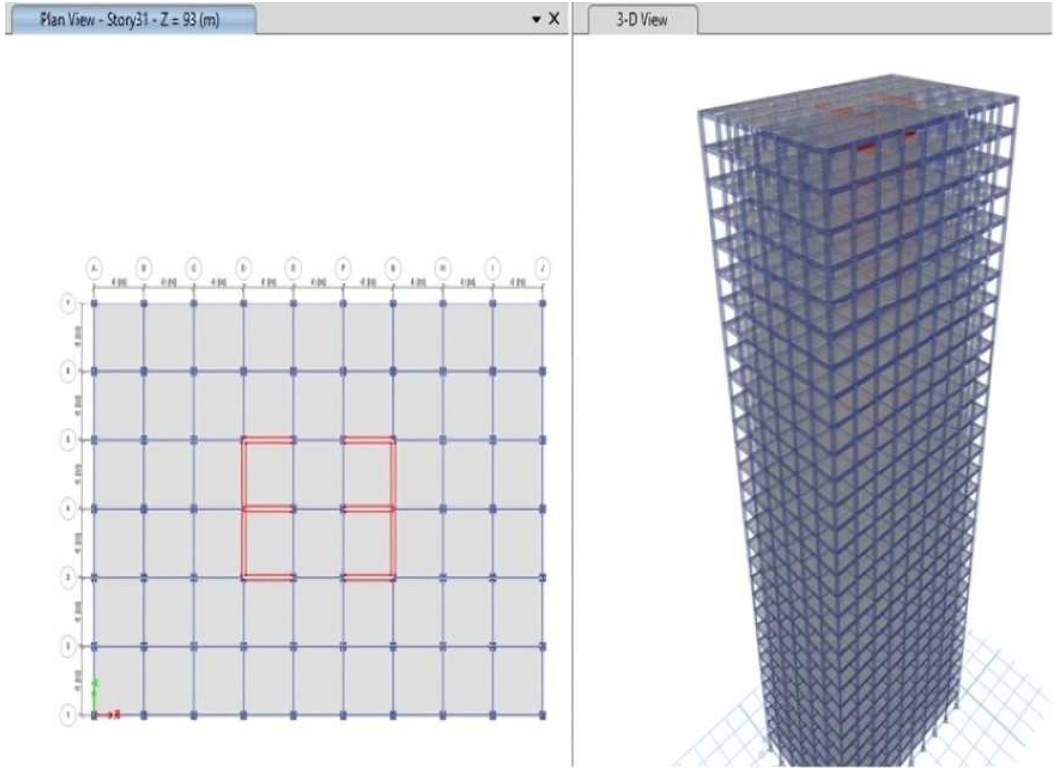


Fig. 8 Simulation 8 - Structure incorporating a centrally positioned shear wall in an E-shaped configuration

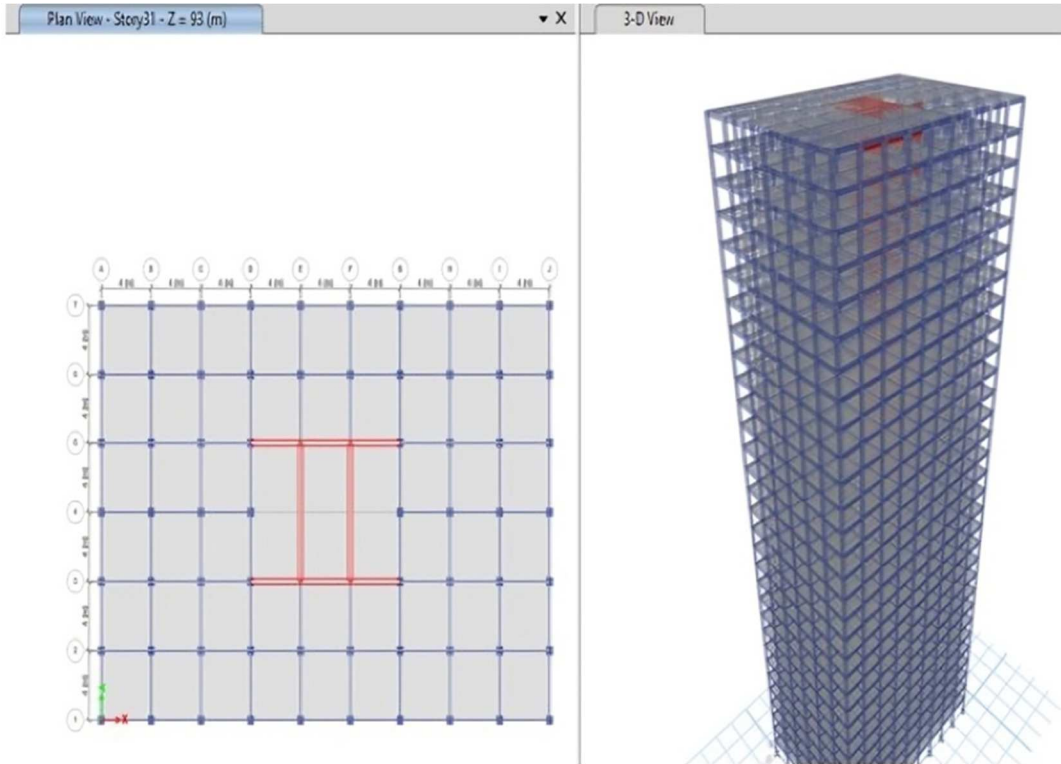


Fig. 9 Simulation 9 - Structure incorporating a centrally positioned shear wall in an I-shaped configuration

Table 1 Geometric parameters

Quantity of lanes in the x - plane	Nine
Quantity of lanes in the y - plane	Six
Length of each bay (meters)	Four
Elevation of each level (m)	Three
Aggregate elevation of structures (m)	93
Dimensions of the beam (mm x mm)	300 x 450
Dimensions of column (mm x mm)	500 x 500
The slab thickness (mm)	150
The shear wall thickness (mm)	300

2.2 MATERIAL PROPERTIES EIGENVALUE PROBLEM FOR SYSTEM

The distinct features of steel and concrete are incorporated into the analysis tool for evaluation. Concrete is regarded as homogeneous, isotropic, and elastic. The properties of both materials utilized in the simulation are presented in Table 2.

Table 2 Characteristics of materials

Material	Steel	Concrete
Grade	Fe415	
Specific weight γ (kN/m ³)	7.697×10^{01}	25
Density ρ (kg/m ³)	7.84905×10^{03}	2.54929×10^3
Modulus of elasticity E (MPa)	0.2×10^{06}	0.274×10^5
Poisson's ratio μ	-----	0.2
Coefficient of thermal expansion (1/°C)	11.7×10^{-04}	0.55×10^{-07}
Shear modulus G (MPa)	-----	0.114×10^{-05}

2.3 EIGENVALUE PROBLEM FOR SYSTEM MODAL DIRECTIONAL FACTOR

The overall formula governing motion associated with an undamped, free-vibration system may be expressed [18] as:

$$[\mathbf{M}] \{\ddot{\delta}\} + [\mathbf{K}] \{\delta\} = 0 \quad (1)$$

Where $[\mathbf{K}]$ and $[\mathbf{M}]$ represent the global stiffness and mass matrix after imposing boundary constraints.

Both the natural frequencies and mode shapes can be determined by solving homogeneous linear Eq. (1) assuming constant coefficients.

Applying the principle of differential equations, it may be shown that the general solution of Eq. (1), assuming harmonic vibrations in the normal mode, can be expressed [18] as:

$$\{\delta\} = \{X\} \sin(\omega t + \varphi) \quad (2)$$

Here $\{X\}$ represents a representation the vector of nodal displacement amplitudes, ω denotes the circular (angular) natural frequency of oscillation [rad/sec], and φ signifies the phase angle.

By substituting Eq. (2) into Eq. (1), the formulas for frequencies and vibrating patterns may be derived, resulting in the standard eigenvalue problem [18]:

$$\{[\mathbf{K}] - \omega^2[\mathbf{M}]\} \{X\} = 0 \quad (3)$$

Equation (3) is solved using a conventional eigenvalue analysis to determine the natural mode shapes and corresponding frequencies of the building model.

3. RESULTS AND DISCUSSION

The free vibration analysis was performed in ETABS software using the eigenvalue method, and the results of parameters such as natural period, corresponding frequency, modal directional factor, and mass participation factor were extracted. As a result, the following section discusses the outcomes of these parameters.

3.1 MODAL PHASE ORIENTED COEFFICIENT

The analysis must be conducted to ensure that the major portion of the building's dead load contributes to the vibration response. Twelve modes were considered until 95 percent of the total mass was engaged. Structures vibrate in various patterns depending on the mode, with three forms of vibration: translational oscillation in the X - direction (U_x), translational oscillation in the Y - direction (U_y), and torsional oscillation (R_z). The modal directional coefficient represents the fraction of vibration that occurs in a specific direction for a given mode. Table 3 presents the directional coefficient for each direction across all modes in Simulation 2. The vibrations of all simulations can be determined using modal directional factor tables, as shown in Table 4. The primary translational direction is depicted in the following table, while negligible portions of oscillation in the alternate direction have been disregarded (e.g., the predominant translational orientation U_y is derived from the first mode of Simulation 2, as illustrated in Table 3, whereas U_x is excluded).

Table 3 Modal directional coefficients for Simulation - 2

Case	Form	U_x	U_y	R_z
Simulation	1	0.009	0.991	0
Simulation	2	0.991	0.009	0
Simulation	3	0	0	1
Simulation	4	0.017	0.983	0
Simulation	5	0.983	0.017	0
Simulation	6	0	0	1
Simulation	7	0.019	0.981	0
Simulation	8	0.98	0.02	0
Simulation	9	0.016	0.984	0
Simulation	10	0	0	1
Simulation	11	0.954	0.046	0
Simulation	12	0.042	0.958	0

Table 4 Vibrating from every simulation in every mode

Form	X- directional Translation	Y- directional Translation	Torsional
1	Simulation - 1,8	Simulation - 2,3,4,5,6,7,9	-----
2	Simulation - 2,3,4,5,6,7	Simulation - 1,8	Simulation - 9
3	Simulation - 9	-----	Simulation - 1,2,3,4,5,6,7,8
4	Simulation - 1,8	Simulation - 2,3,4,5,6,7	Simulation - 9
5	Simulation - 2,3,4,5,6	Simulation - 1,9	Simulation - 7,8
6	Simulation - 7,9	Simulation - 8	Simulation - 1,2,3,4,5,6
7	Simulation - 1	Simulation - 2,3,4,5,6,7	Simulation - 8,9
8	Simulation - 2,3,4,5,8	Simulation - 1,9	Simulation - 6,7
9	Simulation - 6,7	Simulation - 2,4,5,8	Simulation - 1,3,9
10	Simulation - 1,9	Simulation - 3,7	Simulation - 2,4,5,6,8
11	Simulation - 2,3,5,8	Simulation - 1,4,6	Simulation - 7,9
12	Simulation - 4,7	Simulation - 2,3,5,9	Simulation - 1,6,8

Figures 10 to 21 depict the mode shape patterns of oscillation for a single structure (Simulation - 2), providing a clear illustration of the vibration behaviour.

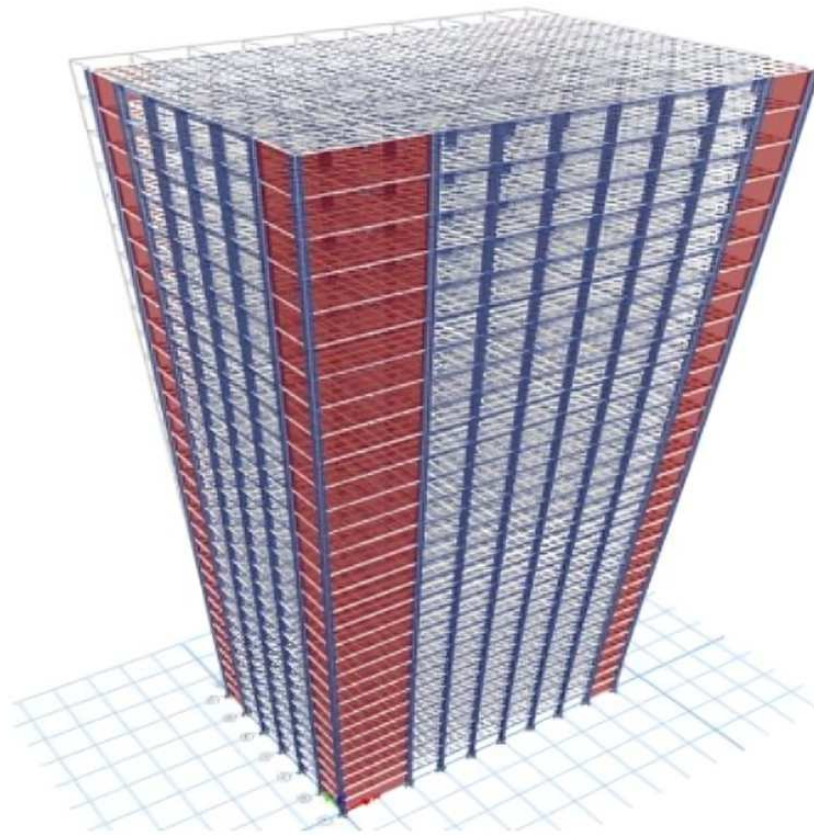


Fig. 10 Form-1 (in the beginning mode of Y directional displacement), $f = 0.37$ Hz

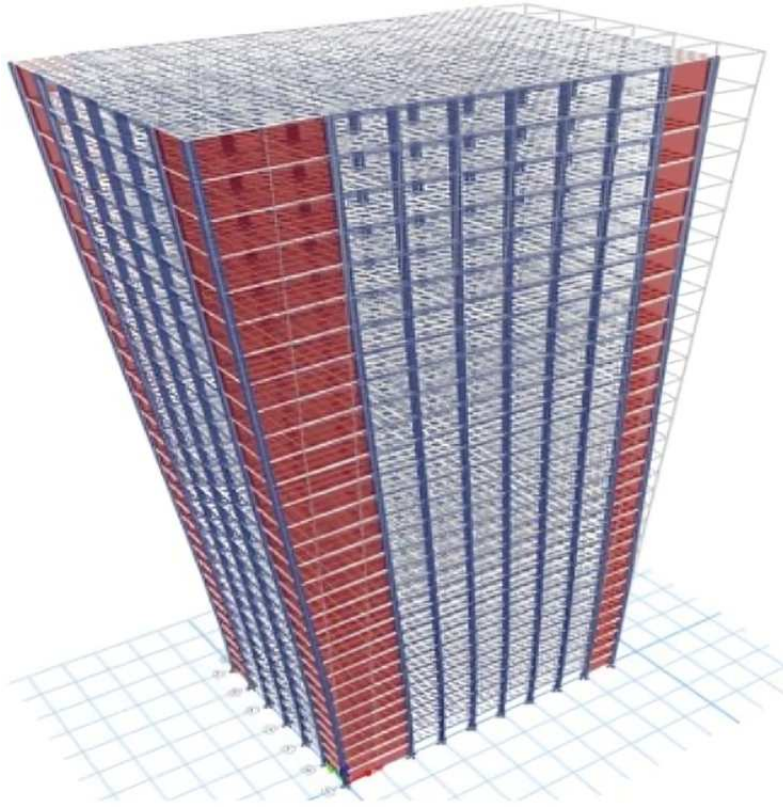


Fig. 11 Form-2 (1st form of X- orientation displacement), $f=0.45$ Hz

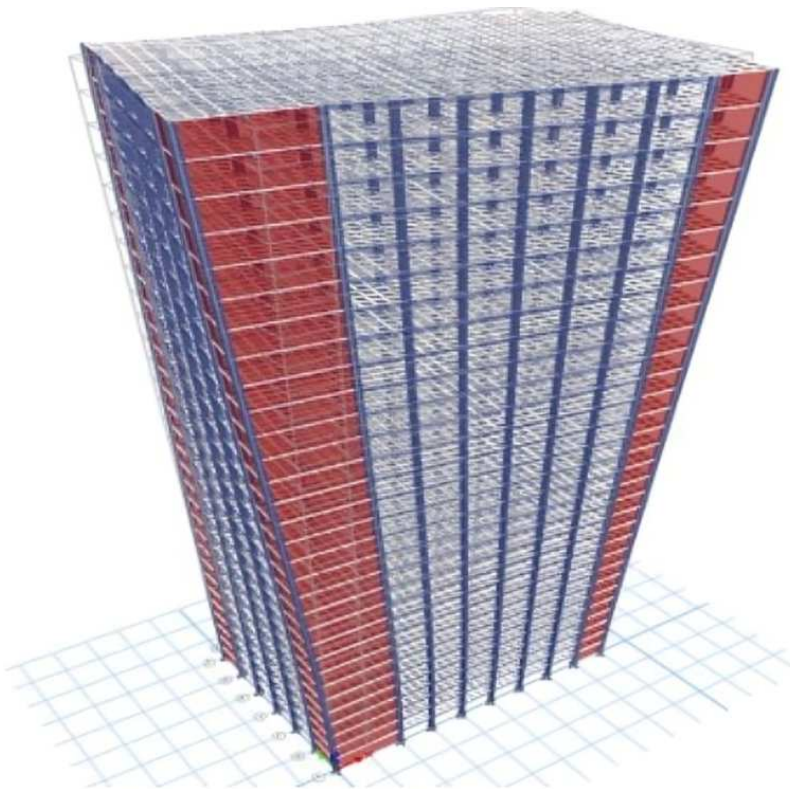


Fig. 12 Mode 3 (first torsional mode), $f=0.54$ Hz

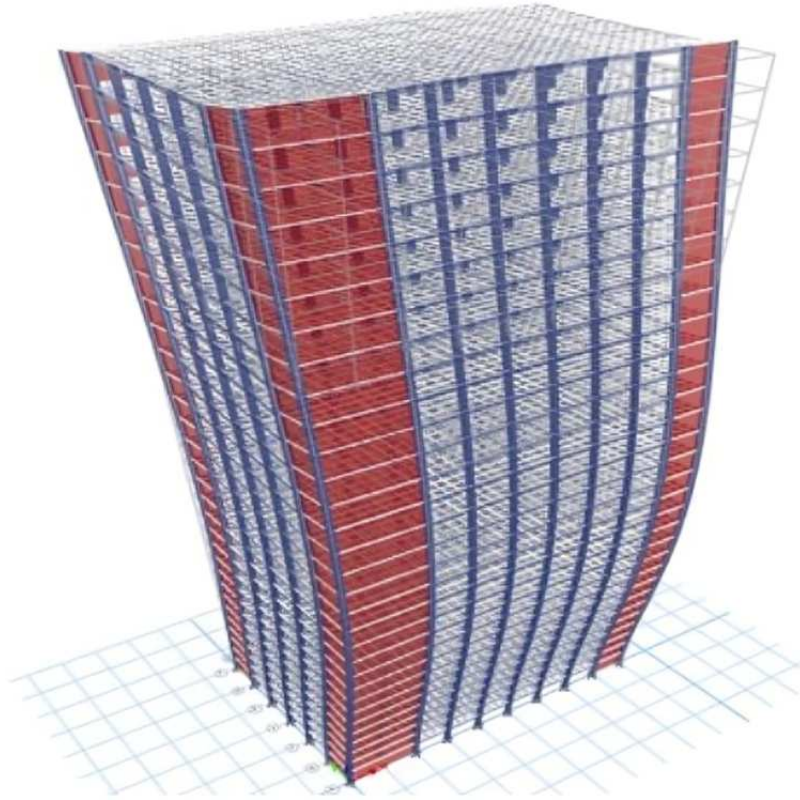


Fig. 13 Mode 4 (second Y-directional displacement mode), $f=1.28$ Hz

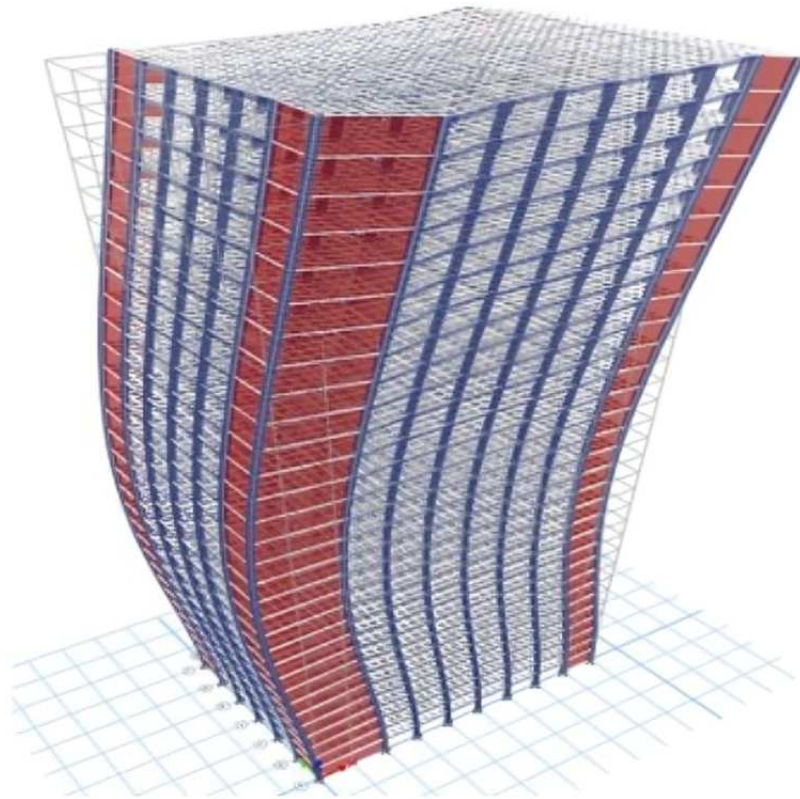


Fig. 14 Mode 5 (second X-directional displacement mode), $f=1.68$ Hz

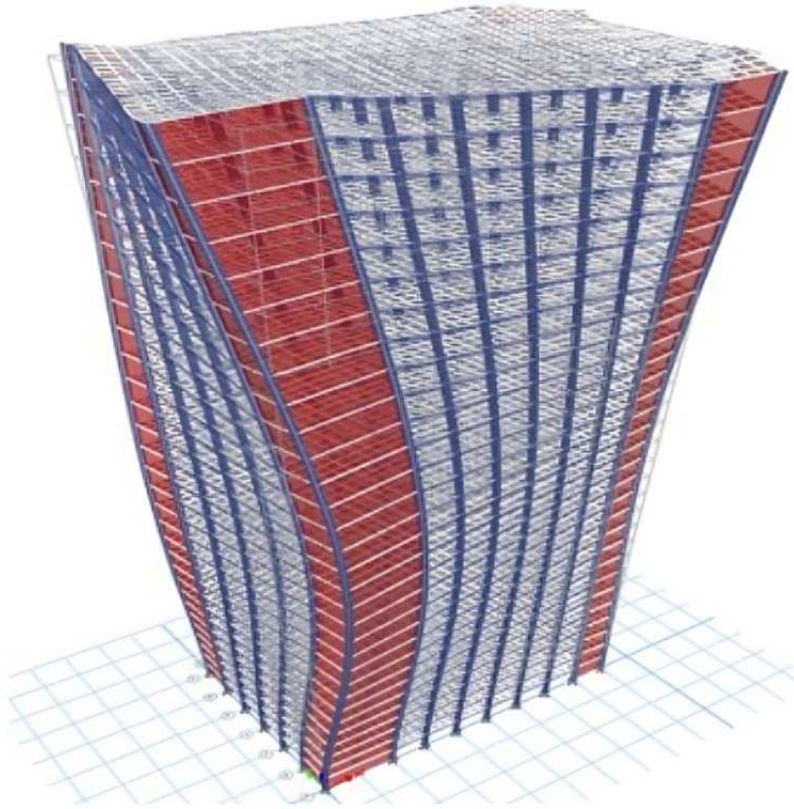


Fig. 15 Mode 6 (second torsional mode), $f=2.12$ Hz

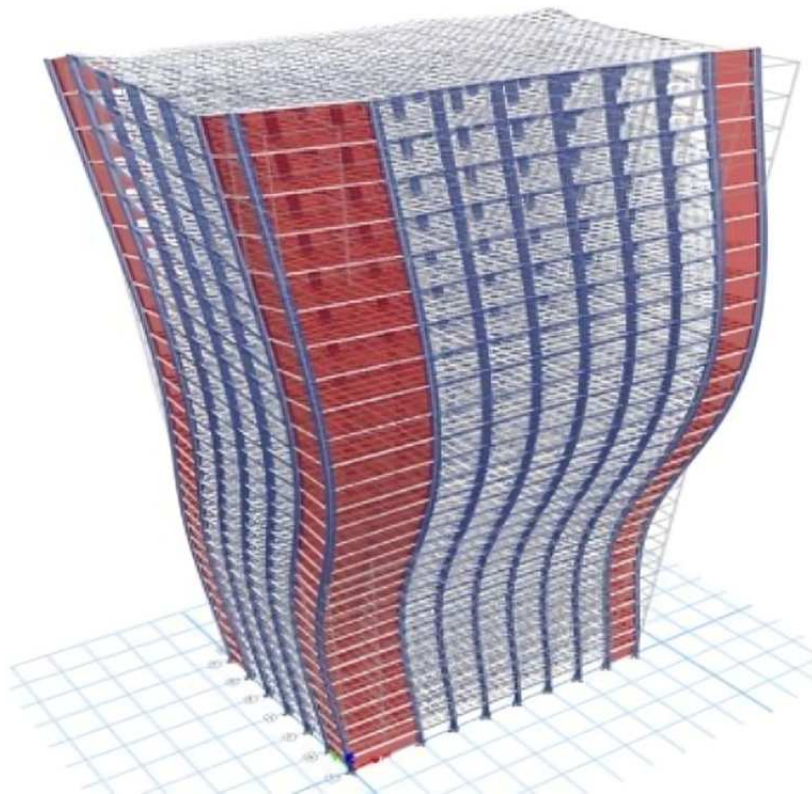


Fig. 16 Mode 7 (third Y-directional displacement mode), $f=2.60$ Hz

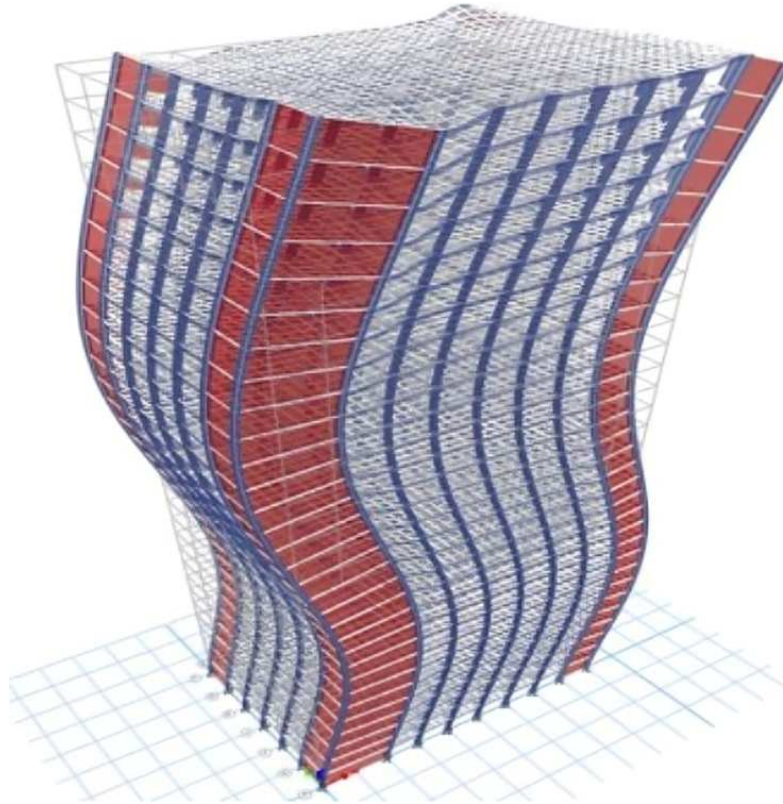


Fig. 17 Mode 8 (third X-directional displacement mode), $f=3.67$ Hz

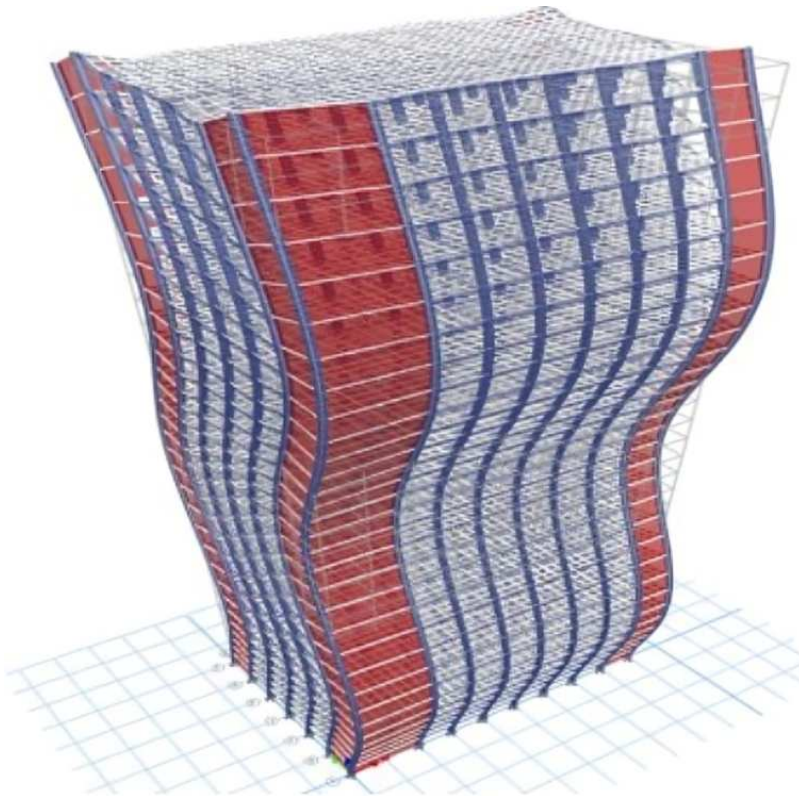


Fig. 18 Mode 9 (fourth Y-directional displacement mode), $f=4.31$ Hz

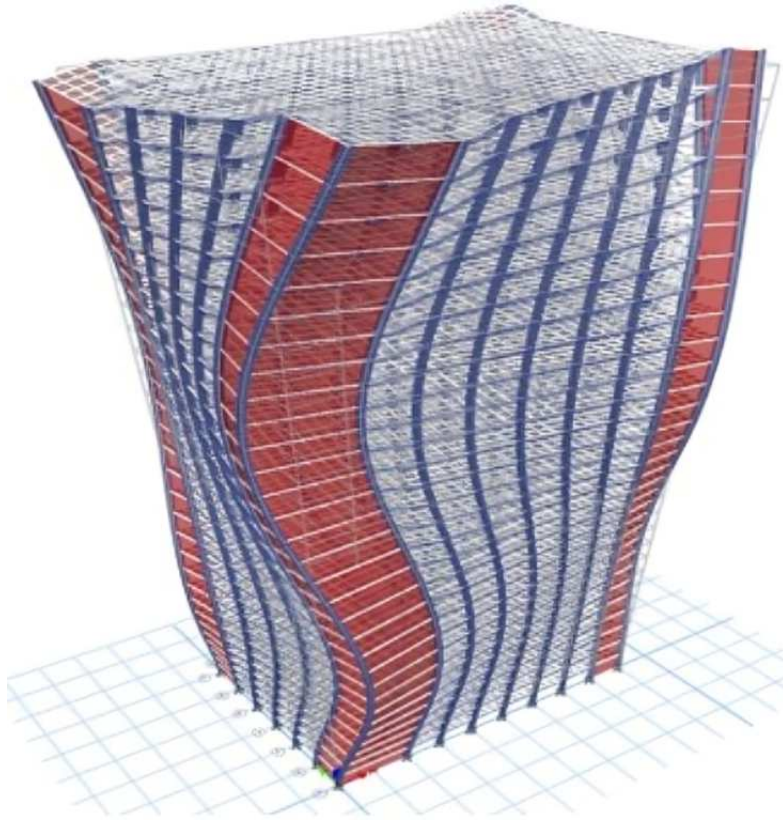


Fig.19 Mode 10 (third torsional mode), $f=4.85$ Hz

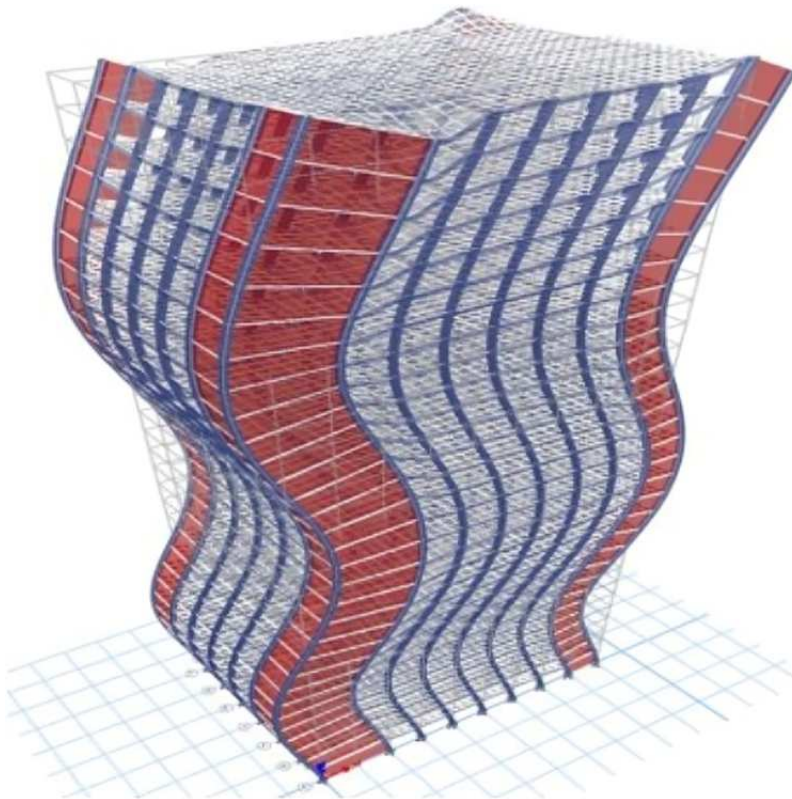


Fig. 20 Mode 11 (fourth X-directional displacement mode), $f=6.20$ Hz

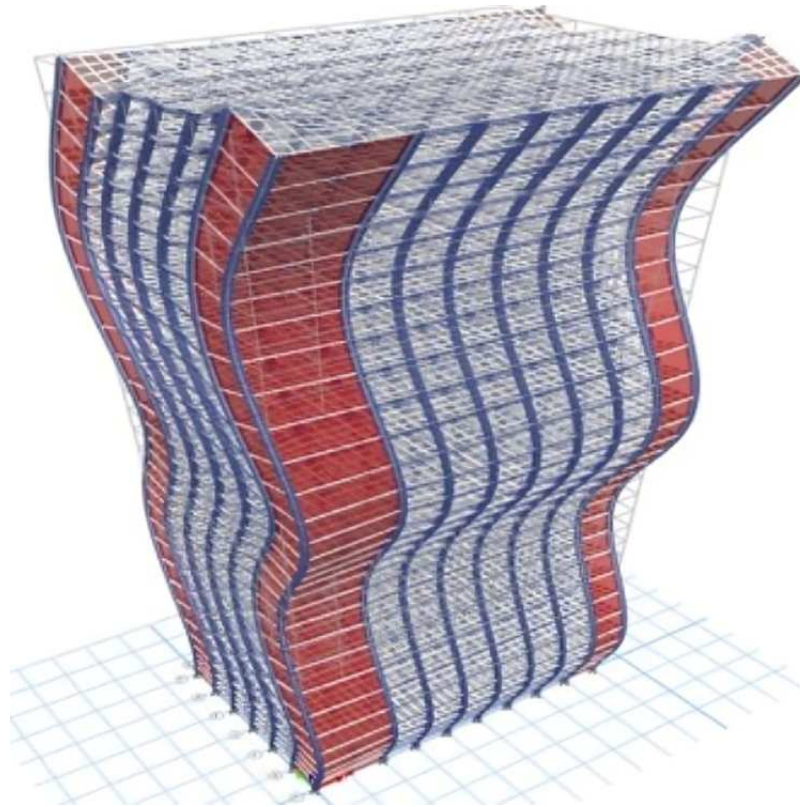


Fig. 21 Mode 12 (fifth Y-directional displacement mode), $f=6.37$ Hz

3.2 MASS ENGAGEMENT INDEX

In the initial phase, mass engagement fluctuates around 65 and 70% for each simulation in their primary mode of vibration. By the 6th mode, approximately 85% of the total mass engagement in the U_x and U_y directions across all simulations. Consequently, these represent the dominant vibration patterns. By the 12th mode, roughly 95% of the mass is engaged in each of the vibration direction throughout whole simulation. Tables 5 and 6 present the total mass engagement for the 1st, 6th, and 12th modes for each simulation in the U_x and U_y directions.

Table 5 Mass engagement rate

Form	Simulation - 1		Simulation - 2		Simulation - 3		Simulation - 4		Simulation - 5	
	U_x	U_y	U_x	U_y	U_x	U_y	U_x	U_y	U_x	U_y
1	0	78.14	0.66	71.79	0.02	71.09	5.38	65.23	0	71.26
2	79.28	78.14	69.82	72.36	68.72	71.11	68.06	69.8	69.32	71.26
3	79.28	78.14	69.82	72.36	68.72	71.11	68.06	69.8	69.32	71.26
4	79.28	89.77	69.99	84.63	68.72	84.49	69.47	82.05	69.32	84.68
5	89.92	89.77	84.18	84.92	84.12	84.49	84.8	84.69	84.31	84.68
6	89.92	89.77	84.18	84.92	84.12	84.49	84.8	84.69	84.31	84.68
12	95.14	95.1	93.35	94.76	93.67	95.04	94.53	95.33	93.7	95.07

Table 6 Mass engagement percentage

Form	Simulation - 6		Simulation - 7		Simulation - 8		Simulation - 9	
	U_x	U_y	U_x	U_y	U_x	U_y	U_x	U_y
1	0	67.94	0	70.61	72.55	0	0	68.91
2	67.63	67.94	69.62	70.61	72.55	68.34	0	68.91
3	67.63	67.94	69.62	70.61	72.55	68.34	68.9	68.91
4	67.63	85.07	69.62	84.66	84.88	68.34	68.9	68.91
5	85.21	85.07	69.62	84.66	84.88	68.34	68.9	85.83
6	85.21	85.07	84.49	84.66	84.88	85.07	84.55	85.83
12	91.6	94.44	93.75	93.15	92.77	91.17	90.64	94.26

3.3 COMPARATIVE ANALYSIS OF TIME PERIODS (T)

Table 7 presents the results of the time period and corresponding frequencies of various modes in Simulation 2. The time periods of various simulations were evaluated using analogous charts generated in ETABS, as illustrated in Figure 22. The model without shear walls exhibits the longest time period in all modes. The introduction of a shear wall increases the structural stiffness, resulting in a decrease in the natural time period. The time period decreased by approximately 16%, 20%, 25%, 22%, 35%, 20%, 26%, and 33% for Simulations 2, 3, 4, 5, 6, 7, 8, and 9, respectively. Simulation 6 shows a notable reduction of 60-67 % across modes 3 to 12, with the maximum decrease of 66.93 % observed in the 12th mode. Simulation 4 exhibits the largest overall reduction, exceeding among 70% in the 12th mode.

Table 7 Time periods and corresponding frequencies

Case	Form	Period (T)	Frequency (f)	Radial Frequency (ω)	Eigenvalue (λ)
		sec	Hz	rad/sec	rad ² /sec ²
Simulation	1	2.70	0.37	2.33	5.44
Simulation	2	2.24	0.45	2.81	7.87
Simulation	3	1.87	0.54	3.36	11.31
Simulation	4	0.78	1.28	8.04	64.56
Simulation	5	0.60	1.68	10.52	110.75
Simulation	6	0.47	2.12	13.33	177.77
Simulation	7	0.38	2.60	16.35	267.16
Simulation	8	0.27	3.67	23.04	530.80
Simulation	9	0.23	4.31	27.06	732.08
Simulation	10	0.21	4.85	30.50	930.03
Simulation	11	0.16	6.20	38.98	1519.22
Simulation	12	0.16	6.37	40.01	1601.15

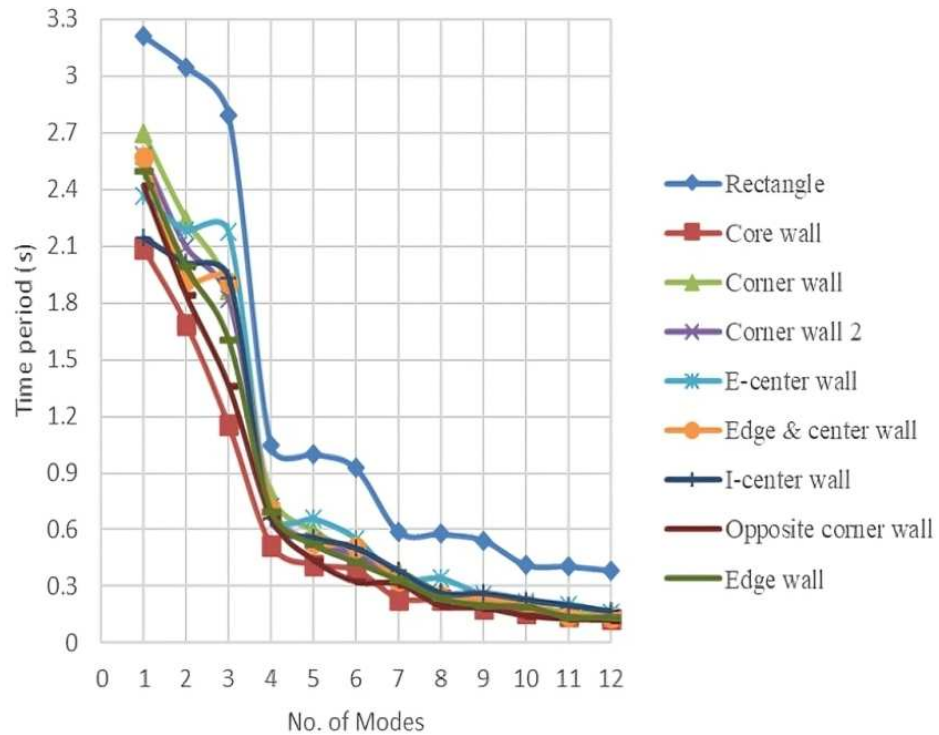


Fig. 22 Comparison of Time Periods

4. CONCLUSIONS

Considering the impact of earthquakes on major structures, tall buildings must be constructed with high precision. Before performing the dynamic (vibration) analysis, it is essential to perform a modal assessment of the building. The present research focused on the modal evaluation of several tall structures, without shear walls. The following points summarize the key findings of this comprehensive analysis:

1. When the stiffness of the structure increases due to the incorporation of a shear wall, the natural time period decreases for all simulations incorporating a shear wall.
2. A centrally positioned shear wall results in a significantly greater reduction in the time period compared with other simulations. The core-type configuration demonstrates the largest reduction in the fundamental mode.
3. Simulations incorporating shear walls placed at all four corners exhibit the least reduction in the time period.

5. NOMENCLATURE

3D - Three - dimensional

2D - Two - dimensional

FEM - Finite Element Method

ETABS - Extended3D Analysis of Building System (Software)

ANSYS - Analysis System

MATLAB - Matrix Laboratory

UQ - Uncertainty Quantification

RCC - Reinforced Cement Concrete

M30 - Concrete grade with a 28-day characteristic strength of 30 N/mm^2

Fe415 - Reinforcement steel with yield strength of 415 N/mm^2

γ - Specific weight

ρ - Density

E - Modulus of elasticity

α - Coefficient of thermal expansion

μ - Poisson's ratio

G - Shear modulus

$[M]$, $[K]$ - Global mass and stiffness matrix

φ - Phase angle

$[\delta]$, $[\ddot{\delta}]$, $[\dot{\delta}]$ - Global displacement, acceleration, and velocity vector matrix values

$[X]$ - Vector of the nodal vibratory amplitude

EI - Flexural stiffness of the cross-section

m - Mass per unit length

L - Length of the beam

U_x , U_y and U_z - Directional translation of X , Y and Z

R_x , R_y and R_z - Rotation of X , Y and Z

T - Time period

f - Cyclic frequency

ω - Circular natural frequency of vibration

λ - Eigenvalue

5. REFERENCES

- [1] Smith, B.S., Coull, A., *Tall Building Structures: Analysis and Design*, New York, John Wiley & Sons, 1991.
- [2] Sultan, M.R., Peera, D.G., Dynamic Analysis of Multi-Storey Building for Different Shapes, *International Journal of Innovative Research in Advanced Engineering*, Vol. 2, No. 8, pp. 85–91, 2015.
- [3] Malekinejad, M., Rahgozar, R., Free vibration analysis of tall buildings with outrigger-belt truss system, *Earthquakes and Structures*, Vol. 2, No. 1, pp. 89–107, 2011.
<https://doi.org/10.12989/eas.2011.2.1.089>
- [4] Fernandez Lorenzo, G.W., Mercerat, D., Santisi d'Avila, M.P., Bertrand, E., Deschamps, A., Operational Modal Analysis of a high rise RC building and modelling, in 6th International operational modal analysis conference (IOMAC 15), Spain, 2015.

Available: <https://hal.science/hal-01143764v1>

- [5] Rahgozar, P., Free vibration of tall buildings using energy method and Hamilton's principle, *Civil Engineering Journal* (Iran), Vol. 6, No. 5, pp. 945–953, 2020.
<https://doi.org/10.28991/cej-2020-03091519>
- [6] Maison, B.F., Ventura, C.E., Dynamic analysis of the thirteen-story building, *Journal of Structural Engineering*, Vol. 117, No. 12, pp. 3783–3803, 1991.
[https://doi.org/10.1061/\(ASCE\)0733-9445\(1991\)117:12\(3783\)](https://doi.org/10.1061/(ASCE)0733-9445(1991)117:12(3783))
- [7] Özyiğit, H.A., Linear vibrations of frames carrying a concentrated mass, *Mathematical and Computational Applications*, Vol. 14, No. 3, pp. 197–206, 2009.
<https://doi.org/10.3390/mca14030197>
- [8] Awkar, J.C., Lui, E.M., Seismic analysis and response of multistory semirigid frames, *Engineering Structures*, Vol. 21, No. 5, pp. 425–441, 1999.
[https://doi.org/10.1016/S0141-0296\(97\)00210-1](https://doi.org/10.1016/S0141-0296(97)00210-1)
- [9] Kwon, Y.W., Bang, H.C., *The Finite Element Method Using MATLAB*, 2nd edition, CRC Press, Boca Raton, 2018. <https://doi.org/10.1201/9781315275949>
- [10] Jang, S.K., Bert, C.W., Free vibration of stepped beams: Exact and numerical solutions, *Journal of Sound and Vibration*, Vol. 130, No. 2, pp. 342–346, 1989.
[https://doi.org/10.1016/0022-460X\(89\)90561-0](https://doi.org/10.1016/0022-460X(89)90561-0)
- [11] Blevins, R.D., Plunkett, R., Formulas For Natural Frequency and Mode Shape, *Journal of Applied Mechanics*, Vol. 47, No. 2, pp. 461–462, 1980. <https://doi.org/10.1115/1.3153712>
- [12] Klein, L., Transverse vibrations of non-uniform beams, *Journal of Sound and Vibration*, Vol. 37, No. 4, pp. 491–505, 1974. [https://doi.org/10.1016/S0022-460X\(74\)80029-5](https://doi.org/10.1016/S0022-460X(74)80029-5)
- [13] Gladwell, G.M.L., The vibration of frames, *Journal of Sound and Vibration*, Vol. 1, No. 4, pp. 402–425, 1964. [https://doi.org/10.1016/0022-460X\(64\)90056-2](https://doi.org/10.1016/0022-460X(64)90056-2)
- [14] Verma, V., Mallothu, A., Nallasivam, K., Modal Analysis of a Thin-Walled Box - Girder Bridge and Railway Track Using Finite Element Framework, *Computational Engineering and Physical Modeling* (CEPM) Vol. 4, No. 4, pp. 64–83, 2021.
- [15] Verma, V., Nallasivam, K., Free vibration behaviour of thin-walled concrete box-girder bridge using Perspex sheet experimental model, *Journal of Achievements in Materials and Manufacturing Engineering*, Vol. 106, No. 2, pp. 56–76, 2021.
<https://doi.org/10.5604/01.3001.0015.2418>
- [16] Verma, V., Nallasivam, K., Static response of curved steel thin-walled box-girder bridge subjected to Indian railway loading, *Journal of Achievements in Materials and Manufacturing Engineering*, Vol. 108, No. 2, pp. 63–74, 2021.
<https://doi.org/10.5604/01.3001.0015.5065>
- [17] ETABS, *Computer & Structures, Inc.: Structural and Earthquake Engineering Software*, 2016. [Online]. Available: <http://www.csiamerica.com/>
- [18] Chopra, A.K., *Dynamics of Structures: Theory and Applications to Earthquake Engineering*, New Jersey, Prentice-Hall, 1995.